

Stability of Thin-Shell Wormholes in Nonlinear Electrodynamics

Muhammad SHARIF¹ *and Muhammad AZAM^{1,2} †

¹ Department of Mathematics, University of the Punjab,
Quaid-e-Azam Campus, Lahore-54590, Pakistan.

² Division of Science and Technology, University of Education,
Township Campus, Lahore-54590, Pakistan.

Abstract

In this paper, we construct thin-shell wormholes by applying the cut and paste procedure to a regular charged black hole in nonlinear electrodynamics field. We discuss different physical aspects of wormholes such as, the possible equation of state to matter shell, attractive or repulsive nature of wormhole and total amount of exotic matter required. The thin-shell equation of motion with and without cosmological constant is also investigated under linearized perturbation. Finally, we explore the stability regions interpreted by the parameter β (speed of sound) and conclude that there are realistic stability regions for some fixed values of parameters.

Keywords: Thin-shell wormholes; Stability; Nonlinear electrodynamics.

PACS: 04.20.Gz; 04.20.Jb; 04.70.Bw.

1 Introduction

Traversable and thin-shell wormholes physics has received great attention due to many astrophysical phenomenon¹⁻³. The idea of traversable wormhole (a

*msharif.math@pu.edu.pk

†azammath@gmail.com

solution of the field equations with two asymptotically flat regions connected by a throat) was suggested by Morris and Thorne⁴⁾. The physical evidence of wormholes has always remained a great problem due to the existence of exotic matter around the throat. However, it was proposed that the amount of exotic matter can be minimized by choosing suitable geometry of the wormhole⁵⁾. The class of thin-shell wormholes are physically interesting, obtained from two manifolds by cut and paste technique^{6,7)}.

The stability of wormholes against perturbations is an interesting issue. Stability of static wormholes has been investigated by using specific equation of state (EoS) or by considering a linearized radial perturbations around a static solution. In this context, Visser⁶⁾, Poisson and Visser⁸⁾ carried out a linearized analysis of the Schwarzschild thin-shell wormhole. Ishak and Lake⁹⁾ studied stability of thin-shell wormholes and found stable solutions. Armendariz-Picon¹⁰⁾ explored stable solution of spherically symmetric configuration against linear perturbations, whereas Shinkai and Hayward¹¹⁾ investigated unstable solution to this class for nonlinear perturbations.

It is found that charge¹²⁾ and positive cosmological constant¹³⁾ increase the stability region in the analysis of linearized stability of spherically symmetric thin-shell wormholes. Thibeault et al.¹⁴⁾ studied stability of thin-shell wormhole in Einstein-Maxwell theory with a Gauss-Bonnet term. Eiroa¹⁵⁾ explored stable and unstable static solutions of spherically symmetric thin-shell wormholes supported by generalized Chaplygin gas. The stability of thin-shell wormholes has been investigated with regular charged black hole¹⁶⁾ and charged black hole in generalized dilaton-axion gravity¹⁷⁾. We have studied the problem of stability for spherical and cylindrical configurations at Newtonian and post-Newtonian approximations and thin-shell wormholes with Chaplygin gas¹⁸⁾.

Besides the lack of observational evidence, wormholes are considered in the family of stars and black holes. For instance, wormhole constructed from two FRW universes can be interpreted as a wormhole with two dynamical stars¹⁹⁾. One can address properties of wormholes and black holes in a unified way such as, black holes being described by a null outer trapped surface and wormholes by a timelike outer trapped surface (throat) where incoming null rays start to diverge²⁰⁾. Wormhole solutions have also been studied in modified theories of gravity. Chodos and Detweiler²¹⁾ and Clement²²⁾ found solutions in higher dimensions, whereas Nandi et. al²³⁾ in Brans-Dicke theory and Shen et. al²⁴⁾ in Kaluza-Klein theory. Kar²⁵⁾ and Anchordoqui and Bergliaffa²⁶⁾ found wormhole solutions in Einstein-Gauss-Bonnet and brane

world scenario respectively.

Born and Infeld²⁷⁾ proposed a specific model based on a principle of finiteness (to avoid physical quantities becoming infinite) in nonlinear electrodynamics. After that, Plebanski²⁸⁾ presented some examples of nonlinear electrodynamics Lagrangians and showed that the Born-Infeld theory satisfies physically acceptable requirements. It is interesting to note that the first exact regular black hole solution in general relativity was found with nonlinear electrodynamics source^{29,30)}. Nonlinear Electrodynamics has been used widely in many applications such as, these theories appear as effective theories at different levels of string theory³¹⁾, explaining the inflationary epoch and the late accelerated expansion of the universe^{32,33)} and the effects produced by nonlinear electrodynamics in spacetimes conformal to Bianchi metrics³⁴⁾. Also, homogenous and isotropic models have been investigated with positive cosmological constant in this scenario³⁵⁾. It was shown that general relativity coupled to nonlinear electrodynamics leads to regular magnetic black holes and monopoles³⁶⁾. The stability of regular electrically charged structures³⁷⁾ with regular de Sitter center has also been explored³⁸⁾. Baldovin et al.³⁹⁾ have shown that an effective wormhole geometry for an electromagnetic wave can appear as a result of the nonlinear character of the field.

The objective of this paper is to construct spherically symmetric thin-shell wormholes from regular charged black hole. To this end, we use the Darmois-Israel thin-shell formalism to derive the thin-shell equation of motion. We discuss various properties of wormholes and investigate its stability regions under linearized radial perturbation. The format of the paper is as follows. Section 2 belongs to overview of the regular charged black hole. Section 3 deals with the mathematical construction of thin-shell wormhole. We discuss EoS relating pressure and density, effect of gravitational field and calculate the total amount of exotic matter in section 4, when cosmological constant is zero. Section 5 is devoted for the stability of wormhole. In section 6, we formulate thin-shell wormholes with cosmological constant and find its stability. Finally, section 7 discusses the results of the paper.

2 Regular Charged Black Hole: An Overview

The study on global regularity of black hole solution is quite important in order to understand the final state of gravitational collapse of initially regu-

lar configurations. None of the regular black holes^{40–43)} (referred to Bardeen black holes) are exact solutions to the Einstein field equations without any physically reasonable source. It is well-known that electrovacuum asymptotically flat metrics endowed with timelike and spacelike symmetries do not allow for the existence of regular black hole solutions. In order to derive regular black hole gravitational nonlinear electromagnetic fields, one has to enlarge the class of electrodynamics to nonlinear ones²⁹⁾. These regular black holes asymptotically behave as ordinary Reissner-Nordström black hole solution and the existence of these solutions does not contradict with the singularity theorems⁴⁴⁾. This motivates us to construct a realistic thin-shell wormhole in nonlinear electrodynamics and investigate its stability.

The action of gravitational field coupled to a nonlinear electrodynamics field with cosmological constant can be defined as⁴⁵⁾

$$S = \frac{1}{4\pi} \int \sqrt{-g} d^4x \left[\frac{1}{4}(R - 2\Lambda) - \mathcal{L}(F) \right], \quad (1)$$

where R is the Ricci curvature of metric $g_{\alpha\beta}$, Λ is the cosmological constant and $\mathcal{L}(F)$ is a gauge-invariant electromagnetic Lagrangian depending on a single invariant $F = \frac{1}{4}F_{\alpha\beta}F^{\alpha\beta}$, where $F_{\alpha\beta} = A_{\beta,\alpha} - A_{\alpha,\beta}$ is the electromagnetic tensor. It is worth mentioning that nonlinear electrodynamics source in the weak field limit becomes the Maxwell field, i.e., $\mathcal{L}(F) = -\frac{F}{4\pi}$. Using the dual transformation,

$$\{g_{\alpha\beta}, F_{\alpha\beta}, F, \mathcal{L}(F)\} \leftrightarrow \{g_{\alpha\beta}, *P_{\alpha\beta}, -P, -\mathcal{H}(P)\}$$

where $*$ is a Hodge operator and $P = \frac{1}{4}P_{\alpha\beta}P^{\alpha\beta} = (\mathcal{L}_F)^2 F$ with $P_{\alpha\beta} = \mathcal{L}_F F_{\alpha\beta}$ an antisymmetric tensor and $\mathcal{L}_F = \frac{d\mathcal{L}}{dF}$, the Hamiltonian \mathcal{H} as a function of P can be written as

$$d\mathcal{H} = (\mathcal{L}_F)^{-1} d[(\mathcal{L}_F)^2 F] = \mathcal{H}_P dP.$$

Also, the Legendre transformation for Hamiltonian \mathcal{H} and Lagrangian \mathcal{L} is⁴⁶⁾

$$\mathcal{H} = 2F\mathcal{L}_F - \mathcal{L}, \quad \mathcal{L} = 2P\mathcal{H}_P - \mathcal{H}.$$

Einstein nonlinear electrodynamics field equations and Bianchi identities in F and P are given, respectively, as follows

$$G_{\alpha\beta} = 2[\mathcal{L}_F F_{\alpha}^{\mu} F_{\beta\mu} - g_{\alpha\beta}(\mathcal{L} + \frac{1}{2}\Lambda)], \quad (2)$$

$$\nabla_{\alpha}(\mathcal{L}_F F^{\alpha\mu}) = 0, \quad \nabla_{\alpha} * F^{\alpha\mu} = 0, \quad (3)$$

$$G_\alpha^\beta = 2[\mathcal{H}_P P_{\alpha\lambda} P^{\beta\lambda} - \delta_\alpha^\beta (2P\mathcal{H}_P - \mathcal{H} + \frac{1}{2}\Lambda)], \quad (4)$$

$$\nabla_\alpha P^{\alpha\mu} = 0, \quad \nabla_\alpha (*\mathcal{H}_P P^{\alpha\mu}) = 0. \quad (5)$$

The specific function determining the nonlinear electromagnetic source is

$$\mathcal{H}(P) = P \frac{(1 - 3\sqrt{-2Q^2 P})}{(1 + \sqrt{-2Q^2 P})^3} - \frac{3}{2Q^2 s} \left(\frac{\sqrt{-2Q^2 P}}{(1 + \sqrt{-2Q^2 P})} \right)^{\frac{5}{2}}.$$

The corresponding nonlinear electromagnetic Lagrangian for the action (1) in F and P frameworks becomes⁴⁵⁾

$$\mathcal{L}(F) = F \frac{(1 - 3\sqrt{2Q^2 F})}{(1 + \sqrt{2Q^2 F})^3} + \frac{3}{2Q^2 s} \left(\frac{\sqrt{2Q^2 F}}{1 + \sqrt{2Q^2 F}} \right)^{\frac{5}{2}},$$

$$\mathcal{L}(P) = P \frac{(1 - 8\sqrt{-2Q^2 P} - 6Q^2 P)}{(1 + \sqrt{-2Q^2 P})^4} - \frac{3}{4Q^2 s} \frac{(-2Q^2 P)^{\frac{5}{4}} (3 - 2\sqrt{-2Q^2 P})}{(1 + \sqrt{-2Q^2 P})^{\frac{7}{2}}},$$

where $s = \frac{|Q|}{2M}$, M and Q are free parameters which would correspond to mass and charge respectively.

Next, we obtain a compatible solution for the $\mathcal{L}(F)$. For this purpose, we consider a static spherically symmetric configuration

$$\mathbf{g} = - \left(1 - \frac{2m(r)}{r} \right) dt^2 + \left(1 - \frac{2m(r)}{r} \right)^{-1} dr^2 + r^2 (d\theta^2 + \sin^2 \theta d\phi^2). \quad (6)$$

Integration of the first of Eq.(5) with the ansatz for the antisymmetric field $P_{\alpha\beta} = 2\delta_{[\alpha}^t \delta_{\beta]}^r D(r)$ yields $P = -\frac{Q^2}{2r^4}$, where we have chosen Q as an integration constant which plays the role of charge in the bulk solution. The zero-zero component of Eq.(2) yields

$$m'(r) = r^2 \mathcal{L}(F) + \frac{\Lambda r^2}{2}. \quad (7)$$

Using $F = -P = \frac{Q^2}{2r^4}$ as well as $\mathcal{L}(F)$ in this equation and then integrating, we have

$$m(r) = M - 3MQ^2 \int_r^\infty \frac{Q^2}{(y^2 + Q^2)^{\frac{5}{2}}} dy - \frac{Q^2}{2} \int_r^\infty \frac{(y^4 - 3Q^2 y^2)}{(y^2 + Q^2)^3} dy + \frac{\Lambda r^3}{6}, \quad (8)$$

where we have used $M = \lim_{r \rightarrow \infty} m(r)$. After integration, it follows that

$$m(r) = \frac{Mr^3}{(r^2 + Q^2)^{\frac{3}{2}}} - \frac{Q^2 r^3}{2(r^2 + Q^2)^2} + \frac{\Lambda r^3}{6}. \quad (9)$$

Inserting $m(r)$ in Eq.(6), we find a solution compatible with the Lagrangian $\mathcal{L}(F)$ as follows

$$ds^2 = -f(r)dt^2 + f^{-1}(r)dr^2 + r^2(d\theta^2 + \sin^2 \theta d\phi^2), \quad (10)$$

where $f(r) = 1 - \frac{2Mr^2}{(r^2 + Q^2)^{\frac{3}{2}}} + \frac{Q^2 r^2}{(r^2 + Q^2)^2} - \frac{\Lambda r^2}{3}$ is a positive function for the given radius.

Now we show that this solution satisfies the weak energy condition. The stress-energy tensor from Eq.(2) can be written as

$$T_{\alpha\beta} = F_{\alpha\gamma}F_{\beta}^{\gamma}\mathcal{L}_F - g_{\alpha\beta}\mathcal{L}(F), \quad (11)$$

where the electromagnetic field tensor defined as

$$F_{\alpha\beta} = E(r)(\delta_{\alpha}^t \delta_{\beta}^r - \delta_{\alpha}^r \delta_{\beta}^t).$$

The invariant F can then be written as

$$2F = -E^2(r), \quad (12)$$

which shows that the electric field can be expressed in terms of the invariant F . To deal with the physically reasonable theories, the fulfillment of the weak energy condition is sufficient for the corresponding energy-momentum tensor. For this, one requires $T_{\alpha\beta}u^{\alpha}u^{\beta} \geq 0$ and $Q_{\alpha}Q^{\alpha} \leq 0$, where $Q^{\alpha} = T_{\beta}^{\alpha}u^{\beta}$ for timelike vector $u^{\alpha} = \frac{\delta_t^{\alpha}}{\sqrt{-g_{tt}}}$. The first inequality implies

$$(\mathcal{L} + E^2\mathcal{L}_F) \geq 0,$$

which becomes $\mathcal{L} \geq E\mathcal{L}_E$ using Eq.(12). The second inequality becomes

$$-(\mathcal{L} + E^2\mathcal{L}_F)^2 \leq 0,$$

which shows that norm of the energy flux Q^{α} occurs to be less than zero.

3 Thin-Shell Wormhole

For the mathematical construction of thin-shell wormhole, we cut two identical 4D copies of the regular charged black hole as

$$\mathcal{M}^\pm = \{x^\gamma = (t, r, \theta, \phi) \mid r \geq a\}, \quad (13)$$

where ‘ a ’ is the throat radius. We paste these geometries at the timelike hypersurface $\Sigma = \Sigma^\pm = \{r - a = 0\}$ to get a new geodesically complete manifold $\mathcal{M} = \mathcal{M}^+ \cup \mathcal{M}^-$ with matter shell at $r = a$. The resulting manifold describes a wormhole with two regions connected by a throat radius placed in the joining shell satisfying the flare-out condition⁴⁷⁾.

We follow the standard Darmois-Israel formalism^{48,49)} to understand the dynamics of the wormhole. The induced metric with throat radius as a function of proper time on Σ is defined as

$$ds^2 = -d\tau^2 + a^2(\tau)(d\theta^2 + \sin^2\theta d\phi^2). \quad (14)$$

The two sides of the shell are matched through the extrinsic curvature defined on Σ as

$$K_{ij}^\pm = -n_\gamma^\pm \left(\frac{\partial^2 x_\pm^\gamma}{\partial \xi^i \partial \xi^j} + \Gamma_{\mu\nu}^\gamma \frac{\partial x_\pm^\mu}{\partial \xi^i} \frac{\partial x_\pm^\nu}{\partial \xi^j} \right), \quad (i, j = 0, 2, 3), \quad (15)$$

where $\xi^i = (\tau, \theta, \phi)$ are the coordinates with τ as the proper time on the shell and n_γ^\pm are the unit normals satisfying the relation $n^\gamma n_\gamma = 1$ to Σ given by

$$n_\gamma^\pm = \left(-\dot{a}, \frac{\sqrt{f(a) + \dot{a}^2}}{f(a)}, 0, 0 \right). \quad (16)$$

Using the orthonormal basis $\{e_{\hat{\tau}} = e_\tau, e_{\hat{\theta}} = a^{-1}e_\theta, e_{\hat{\phi}} = (a \sin \theta)^{-1}e_\phi\}$, the non-vanishing components of the extrinsic curvature turns out to be

$$K_{\hat{\tau}\hat{\tau}}^\pm = \mp \frac{f'(a) + 2\ddot{a}}{2\sqrt{f(a) + \dot{a}^2}}, \quad K_{\hat{\theta}\hat{\theta}}^\pm = K_{\hat{\phi}\hat{\phi}}^\pm = \pm \frac{1}{a} \sqrt{f(a) + \dot{a}^2}. \quad (17)$$

Here dot and prime denote derivatives with respect to τ and a respectively.

The surface stress-energy tensor $S_{\hat{i}\hat{j}} = \text{diag}(\sigma, p_{\hat{\theta}}, p_{\hat{\phi}})$ provides surface energy density σ and surface tensions $p_{\hat{\theta}}, p_{\hat{\phi}}$ of the shell. The Lanczos equations are defined on the shell as

$$S_{\hat{i}\hat{j}} = \frac{1}{8\pi} \{g_{\hat{i}\hat{j}} K - [K_{\hat{i}\hat{j}}]\}, \quad (18)$$

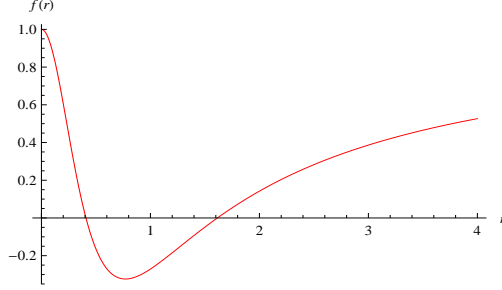


Figure 1: (Color online) $f(r)$ cuts the r -axis at r_- and r_+ (Event horizons) for $Q = 0.5$ and $M = 1$ in the absence of Λ .

where $[K_{ij}] = K_{ij}^+ - K_{ij}^-$ and $K = tr[K_{ij}] = [K_i^i]$. Using Eqs.(17) and (18), the energy density σ and transverse pressure p to shell are obtained as

$$\sigma = -\frac{1}{2\pi a} \sqrt{f(a) + \dot{a}^2}, \quad (19)$$

$$p = p_{\hat{\theta}} = p_{\hat{\phi}} = \frac{1}{8\pi a} \frac{2a\ddot{a} + 2\dot{a}^2 + 2f(a) + af'(a)}{\sqrt{f(a) + \dot{a}^2}}. \quad (20)$$

4 Thin-Shell Wormhole Without Λ

Here we consider the case, when $\Lambda = 0$ for the given metric. It is shown in Fig. 1 that there exist two event horizons for such a black hole, whenever $|Q| \leq 0.6M^{29}$. We explore EoS parameter. The corresponding energy density and surface potential from Eqs.(19) and (20) for static configuration of radius a ($\dot{a} = \ddot{a} = 0$) become

$$\sigma = -\frac{1}{2\pi a} \left[1 - \frac{2Ma^2}{(a^2 + Q^2)^{\frac{3}{2}}} + \frac{Q^2 a^2}{(a^2 + Q^2)^2} \right]^{\frac{1}{2}}, \quad (21)$$

$$p = \frac{\left[1 - \frac{4Ma^2}{(a^2 + Q^2)^{\frac{3}{2}}} + \frac{3Ma^4}{(a^2 + Q^2)^{\frac{5}{2}}} + \frac{2Q^2 a^2}{(a^2 + Q^2)^2} - \frac{2Q^2 a^4}{(a^2 + Q^2)^3} \right]}{4\pi a \left[1 - \frac{2Ma^2}{(a^2 + Q^2)^{\frac{3}{2}}} + \frac{Q^2 a^2}{(a^2 + Q^2)^2} \right]^{\frac{1}{2}}}. \quad (22)$$

In static wormholes, the throat is defined as minimal area surface satisfying

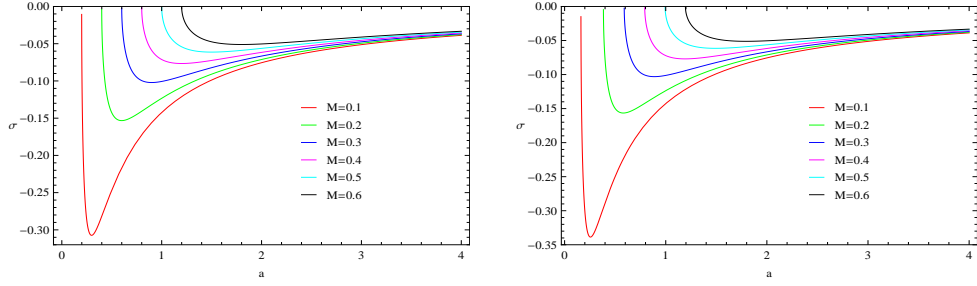


Figure 2: (Color online) Plots of σ versus a with fixed values of $Q = 0.01$ and $Q = 0.05$.

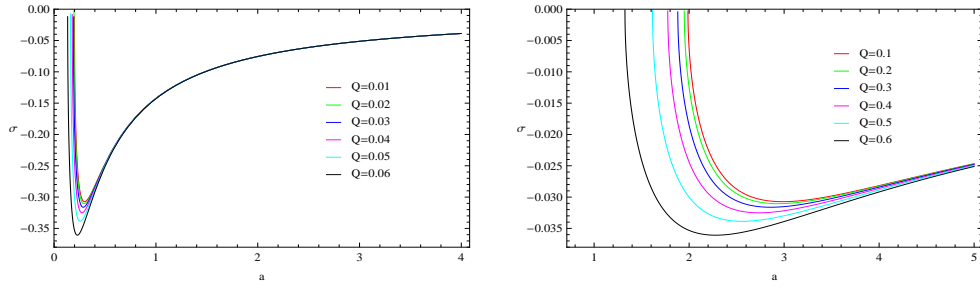


Figure 3: (Color online) Plots of σ versus a with fixed values of $M = 0.1$ and $M = 1$.

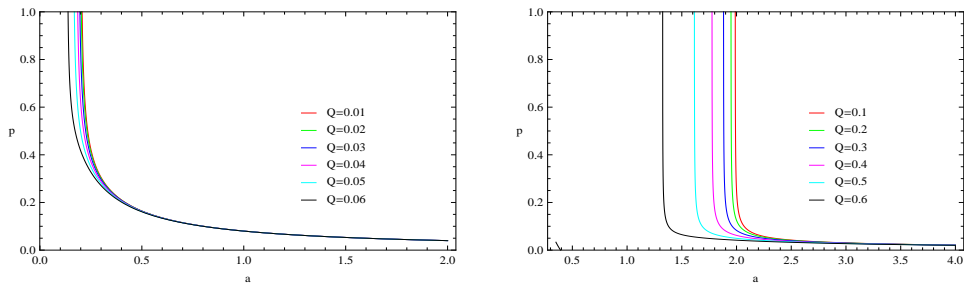


Figure 4: (Color online) Plots of p versus a for fixed values of $M = 0.1$ and $M = 1$.

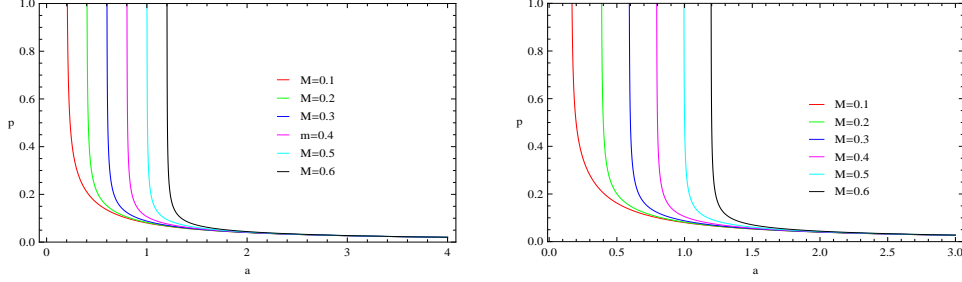


Figure 5: (Color online) Plots of p versus a for fixed value of $Q = 0.01$ and $Q = 0.05$.

the flare-out condition. To fulfill this condition, wormholes must be threaded by the exotic matter (violating the null energy condition (NEC), i.e., $\sigma + p < 0$)^{50,51}. We see from Figs. **2-5** that energy density is negative and pressure is a decreasing function of throat radius for some fixed values of charge and mass. This shows that matter on the shell (violating both NEC and weak energy condition (WEC)) implies the presence of exotic matter. For the explanation of this matter, we consider an EoS on the shell as

$$p = \omega \sigma, \quad (23)$$

where ω is the EoS parameter. Using Eqs.(21) and (22), we have

$$\frac{p}{\sigma} = \omega = -\frac{1}{2} - \frac{\left[-\frac{2Ma^2}{(a^2+Q^2)^{\frac{3}{2}}} + \frac{3Ma^4}{(a^2+Q^2)^{\frac{5}{2}}} + \frac{Q^2a^2}{(a^2+Q^2)^2} - \frac{2Q^2a^4}{(a^2+Q^2)^3} \right]}{2 \left[1 - \frac{2Ma^2}{(a^2+Q^2)^{\frac{3}{2}}} + \frac{Q^2a^2}{(a^2+Q^2)^2} \right]}. \quad (24)$$

We see that $\omega \rightarrow -\frac{1}{2}$, if the location of the wormhole throat is large enough, i.e., $a \rightarrow \infty$. This shows that the distribution of matter in the shell is of dark energy type. We obtain dust shell, i.e., $p \rightarrow 0$ when $a \rightarrow a_0$ (the point where the curve cuts the a -axis shown in the right graph of Fig. **6**) for fixed values of $M = 1$ and $Q = 0.5$. However, $a_0 < r_h$ (in our case), the dust shell can never be found. Also, the Casimir effect with massless field is of traceless type, so the dust shell can be looked into by taking trace of the surface stress-energy tensor, i.e., $S_j^i = 0$ implies that $-\sigma + 2p = 0$, which yields

$$g(a) = 2 - \frac{6Ma^2}{(a^2+Q^2)^{\frac{3}{2}}} + \frac{3Ma^4}{(a^2+Q^2)^{\frac{5}{2}}} + \frac{3Q^2a^2}{(a^2+Q^2)^2} - \frac{2Q^2a^4}{(a^2+Q^2)^3} = 0. \quad (25)$$

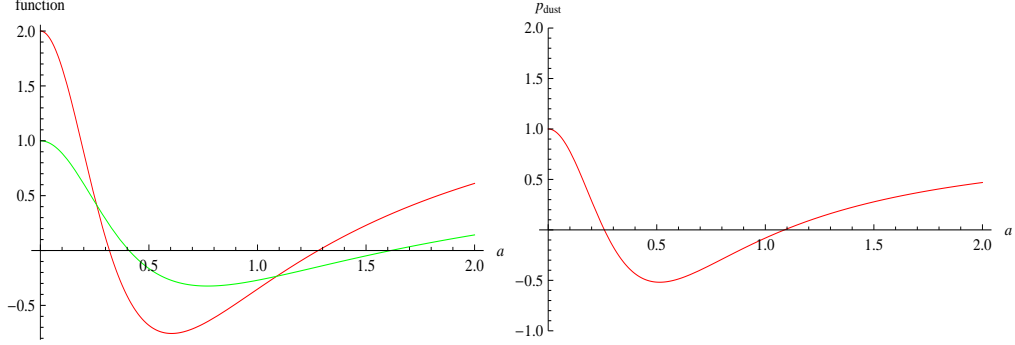


Figure 6: (Color online) The left graph shows the behavior of the function $f(a)$ (green) and $g(a)$ (red) for fixed values of $Q = 0.5$ and $M = 1$.

The left graph of Fig. 6 shows that the red curve cuts the a -axis before the green curve. This shows that throat of the wormhole satisfying the above equation lies inside the event horizon of the black hole, hence not possible in a wormhole configuration. Thus, a dust shell cannot be found.

The Gravitational Field

The gravitational field of wormhole depends upon the observer's four acceleration. The nature of wormhole is attractive or repulsive according to $a^r > 0$ or $a^r < 0$, respectively. The observer's four acceleration is defined as

$$a^\mu = v^\mu_{;\nu} v^\nu, \quad (26)$$

where

$$v^\nu = \frac{dx^\nu}{d\tau} = \left(\frac{1}{\sqrt{f(r)}}, 0, 0, 0 \right).$$

The only non-vanishing component of the four acceleration is

$$a^r = \Gamma^r_{tt} \left(\frac{dt}{d\tau} \right)^2 = \frac{1}{r} \beta(r), \quad (27)$$

where

$$\beta(r) = \left[-\frac{2\frac{M}{r}}{(1 + (\frac{Q}{r})^2)^{\frac{3}{2}}} + \frac{3\frac{M}{r}}{(1 + (\frac{Q}{r})^2)^{\frac{5}{2}}} + \frac{(\frac{Q}{r})^2}{(1 + (\frac{Q}{r})^2)^2} - \frac{2(\frac{Q}{r})^2}{(1 + (\frac{Q}{r})^2)^3} \right]. \quad (28)$$

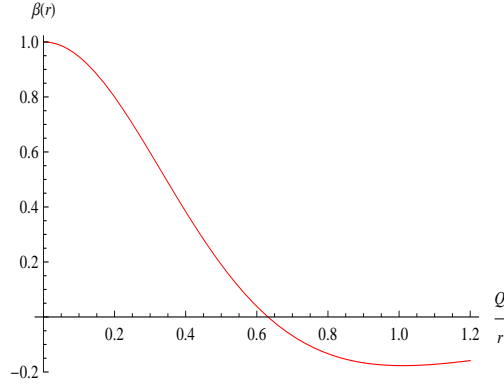


Figure 7: (Color online) Plot of $\beta(r)$ versus $\frac{Q}{r}$: x is the point where the function $\beta(r)$ cuts the $\frac{Q}{r}$ -axis.

Also, the the geodesic equation for a radially moving test particle initially at rest can be defined as

$$a^r = -\frac{d^2 r}{d\tau^2} = -\Gamma_{tt}^r \left(\frac{dt}{d\tau} \right)^2. \quad (29)$$

Figure 7 shows that the curve cuts at the point $x = \frac{Q}{r}$ for a fixed value of $\frac{M}{r} = 1$. Hence, the wormhole will be attractive for $x > \frac{Q}{r}$ and repulsive for $x < \frac{Q}{r}$. We obtain a geodesic equation for $x = \frac{Q}{r}$, i.e., $a^r = 0$.

The Total Amount of Exotic Matter

It is found that the total amount of exotic matter required to support wormholes can be made as small as possible by choosing appropriate geometry of the wormhole⁵⁾. Here, we show that the total amount of exotic matter can be reduced by either increasing the mass or decreasing the charge of the black hole. We consider the integral⁵²⁾

$$\Omega_\alpha = \int (\rho + p) \sqrt{-g} d^3 x. \quad (30)$$

Choosing $R = r - a$ as the radial coordinate, we have

$$\Omega_\alpha = \int_0^{2\pi} \int_0^\pi \int_{-\infty}^\infty (\rho + p) \sqrt{-g} dR d\theta d\phi. \quad (31)$$

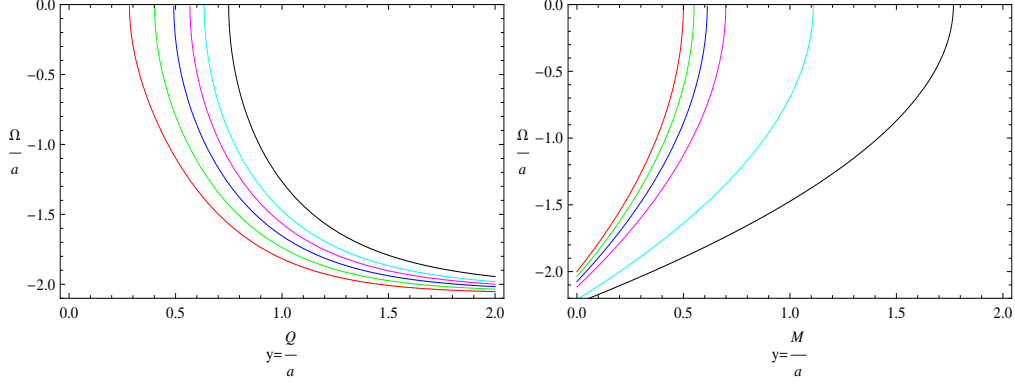


Figure 8: (Color online) Variation in the total amount of exotic matter for $\frac{M}{a} = 0.6, 0.7, 0.8, 0.9, 1, 1.2$ and $\frac{Q}{a} = 0, 0.2, 0.3, 0.4, 0.7, 1$.

The infinitely thin shell does not exert any radial pressure, therefore, using $\rho = \delta(R)\sigma(a)$, it follows that

$$\begin{aligned}\Omega_\alpha &= \int_0^{2\pi} \int_0^\pi \sigma \sqrt{-g}|_{r=a} d\theta d\phi = 4\pi a^2 \sigma(a) \\ &= -2a \left[1 - \frac{2Ma^2}{(a^2 + Q^2)^{\frac{3}{2}}} + \frac{Q^2 a^2}{(a^2 + Q^2)^2} \right]^{\frac{1}{2}}.\end{aligned}\quad (32)$$

The matter violating NEC can be reduced by choosing a closer to r_h . When $a \rightarrow r_h$, the wormhole is closer to a black hole as the incoming microwave background radiation would become blueshifted at a high temperature⁵³). It is observed from Eq.(32) that for $a \gg r_h$, Ω_α will depend linearly upon a , i.e., $\Omega_\alpha \approx -2a$. Figure 8 shows the variation of exotic matter corresponding to mass and charge of the black hole. Thus, the total exotic matter can be reduced by either increasing mass or decreasing charge of the black hole.

5 Stability Analysis

In this section, we obtain the stability regions of the static configuration of wormhole under a small perturbation around the static solution $a = a_0$. For this purpose, we consider thin shell equation of motion (by re-arranging

Eq.(19))

$$\dot{a}^2 + V(a) = 0, \quad (33)$$

where the potential $V(a)$ is given as

$$V(a) = f(a) - [2\pi a\sigma(a)]^2. \quad (34)$$

For the linearized stability criteria, we use Taylor expansion to $V(a)$ upto second order around a_0

$$V(a) = V(a_0) + V'(a_0)(a - a_0) + \frac{1}{2}V''(a_0)(a - a_0)^2 + O[(a - a_0)^3]. \quad (35)$$

The change in the internal energy plus the work done by the internal forces of the throat is equal to the flux term known as energy conservation equation, which can be written with the help of Eqs.(19) and (20) as

$$\frac{d(\sigma\mathcal{A})}{d\tau} + p\frac{d\mathcal{A}}{d\tau} = \{[2a]^2 - 4a\} \frac{\dot{a}\sqrt{f(a) + \dot{a}^2}}{4a}, \quad (36)$$

where $\mathcal{A} = 4\pi a^2$ is the area of the wormhole throat. Using $\sigma' = \frac{\dot{\sigma}}{a}$ in the above equation, we have

$$a^2\sigma' + 2a(\sigma + p) + \{[2a]^2 - 4a\} \frac{\sigma}{4a} = 0. \quad (37)$$

Inserting $(a\sigma)' = -(\sigma + p)$, the first derivative of Eq.(34) can be written as

$$V'(a) = f'(a) + 8\pi^2 a\sigma(\sigma + p). \quad (38)$$

Here, we define a parameter β (velocity of sound), which should be less than one for a realistic model^{54,55)}

$$\beta^2(\sigma) = \frac{\partial p}{\partial \sigma}|_{\sigma}. \quad (39)$$

Notice that

$$\sigma'(a) + 2p'(a) = \sigma'(a) \left[1 + 2\frac{p'(a)}{\sigma'(a)} \right] = \sigma'(a)(1 + 2\beta^2). \quad (40)$$

Using the above equation and taking derivative of Eq.(38), it follows that

$$V''(a) = f''(a) - 8\pi^2(\sigma + 2p)^2 - 8\pi^2 [2\sigma(1 + 2\beta^2)(\sigma + p)]. \quad (41)$$

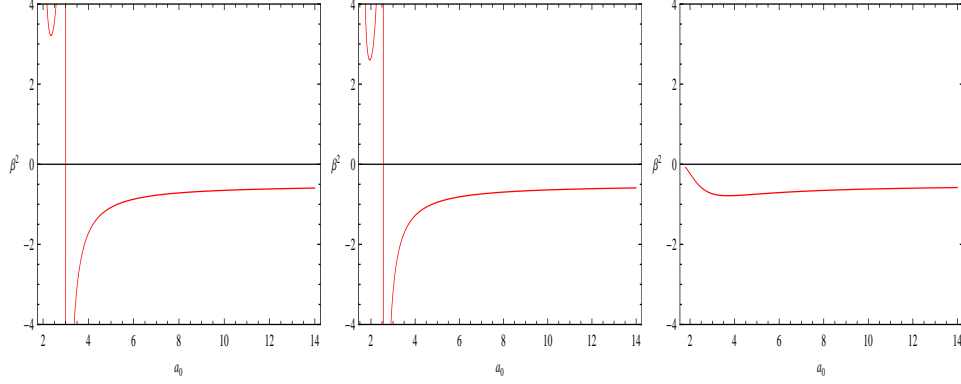


Figure 9: (Color online) Stability regions for thin-shell wormholes corresponding to $Q = 0.1, 0.5, 0.9$ and fixed value of $M = 1$.

For the stable configuration, we require that $V(a_0) = 0 = V'(a_0)$ and $V''(a_0) > 0$. It is easy to see that using Eq.(19) in (20), the potential and its derivative are zero at $a = a_0$. Solving the above equation for β^2 by letting $V''(a_0) = 0$, we have

$$\beta^2 = -\frac{1}{2} + \frac{\frac{f''}{8\pi^2} - (\sigma + 2p)^2}{4\sigma(\sigma + p)}, \quad (42)$$

The graphical representation (Fig. 9) shows the stability regions to the left and right of the asymptote. To the right of asymptote, the stability criterion $V''(a_0) > 0$ leads to the stability region with inequality

$$\beta^2 < -\frac{1}{2} + \frac{\frac{f''}{8\pi^2} - (\sigma + 2p)^2}{4\sigma(\sigma + p)}. \quad (43)$$

However, the sense of inequality for the stability region to the left of the asymptote is reversed as

$$\beta^2 > -\frac{1}{2} + \frac{\frac{f''}{8\pi^2} - (\sigma + 2p)^2}{4\sigma(\sigma + p)}. \quad (44)$$

The regions of stability corresponding to $Q = 0.1, 0.5, 0.9$ for fixed value of $M = 1$ are shown in Fig. 9. It is noted that the stability regions exist under the radial perturbations but do not correspond to the range $0 < \beta^2 \leq 1$ for different values of charge.

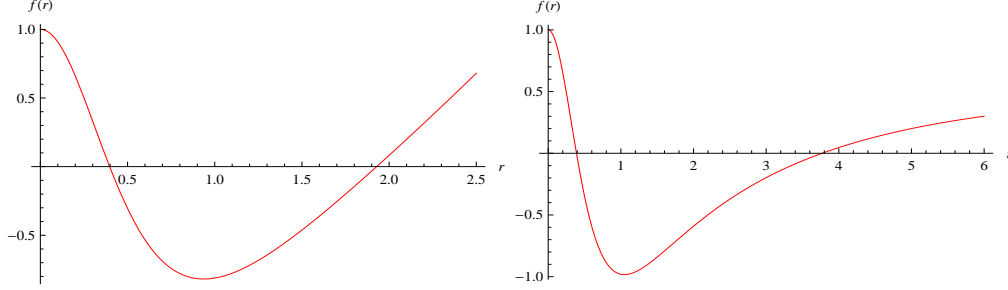


Figure 10: (Color online) Both left and right graphs show event horizons ($f(r)$ cuts the r -axis) for fixed values of $Q = 0.7$ and $M = 2$ corresponding to positive and negative Λ .

6 Thin-Shell Wormhole With Λ

Here, we construct thin-shell wormhole from regular black hole with cosmological constant and find its stability regions for some fixed values of Q , M and Λ . The event horizons for such a black hole are shown in Fig. 10. In this scenario, the surface energy density and surface pressure are

$$\sigma = -\frac{1}{2\pi a} \left[1 - \frac{2Ma^2}{(a^2 + Q^2)^{\frac{3}{2}}} + \frac{Q^2 a^2}{(a^2 + Q^2)^2} - \frac{\Lambda a^2}{3} \right]^{\frac{1}{2}}, \quad (45)$$

$$p = \frac{\left[1 - \frac{4Ma^2}{(a^2 + Q^2)^{\frac{3}{2}}} + \frac{3Ma^4}{(a^2 + Q^2)^{\frac{5}{2}}} + \frac{2Q^2 a^2}{(a^2 + Q^2)^2} - \frac{2Q^2 a^4}{(a^2 + Q^2)^3} - \frac{\Lambda a^2}{3} \right]}{4\pi a \left[1 - \frac{2Mr^2}{(r^2 + Q^2)^{\frac{3}{2}}} + \frac{Q^2 r^2}{(r^2 + Q^2)^2} - \frac{\Lambda a^2}{3} \right]^{\frac{1}{2}}}. \quad (46)$$

Using Eq.(23), the EoS parameter is given as

$$\omega = \frac{p}{\sigma} = -\frac{1}{2} - \frac{\left[-\frac{2Ma^2}{(a^2 + Q^2)^{\frac{3}{2}}} + \frac{3Ma^4}{(a^2 + Q^2)^{\frac{5}{2}}} + \frac{Q^2 a^2}{(a^2 + Q^2)^2} - \frac{2Q^2 a^4}{(a^2 + Q^2)^3} - \frac{\Lambda a^2}{3} \right]}{2 \left[1 - \frac{2Ma^2}{(a^2 + Q^2)^{\frac{3}{2}}} + \frac{Q^2 a^2}{(a^2 + Q^2)^2} - \frac{\Lambda a^2}{3} \right]}. \quad (47)$$

The matter distribution in the shell is of dark energy type similar to the above case, i.e., for $a \rightarrow \infty$, we have $\omega \rightarrow -1$.

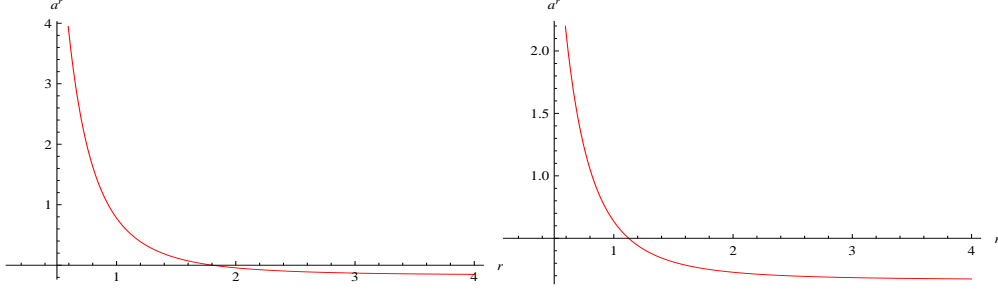


Figure 11: (Color online) Plot of a^r versus radial coordinate for positive and negative cosmological constant.

The corresponding gravitational field will be

$$a^r = \left[-\frac{2Mr}{(r^2 + Q^2)^{\frac{3}{2}}} + \frac{3Mr^3}{(r^2 + Q^2)^{\frac{5}{2}}} + \frac{Q^2 r}{(r^2 + Q^2)^2} - \frac{2Q^2 r^3}{(r^2 + Q^2)^3} - \frac{\Lambda r}{3} \right]. \quad (48)$$

The attractive ($a^r > 0$) and repulsive ($a^r < 0$) behavior of the thin-shell wormhole with cosmological constant is shown in Fig. 11 for fixed values of $M = 1$, $Q = 0.1$, $\Lambda = 0.5$ and $M = 0.5$, $Q = 0.1$, $\Lambda = -0.5$.

The total amount of exotic matter around the throat turns out to be

$$\Omega_\alpha = -2a \left[1 - \frac{2Ma^2}{(a^2 + Q^2)^{\frac{3}{2}}} + \frac{Q^2 a^2}{(a^2 + Q^2)^2} - \frac{\Lambda a^2}{3} \right]^{\frac{1}{2}}. \quad (49)$$

Similar to the above case, the total amount of exotic matter can be reduced by choosing some appropriate fixed values of M , Q and Λ .

Stability Analysis

Using the same procedure as in the absence of cosmological constant, we have stability condition for the thin-shell wormhole in the presence of cosmological constant as

$$\beta^2 = -\frac{1}{2} + \frac{\frac{f''}{8\pi^2} - (\sigma + 2p)^2}{4\sigma(\sigma + p)}, \quad (50)$$

where surface energy density and surface potential are given by Eqs.(45) and (46). The typical regions of stability are shown in Fig. 12 for fixed values of the parameters $M = 2$, $Q = 0.1$, $\Lambda = -0.5$ and $M = 2$, $Q = 0.1$, $\Lambda = -0.9$.

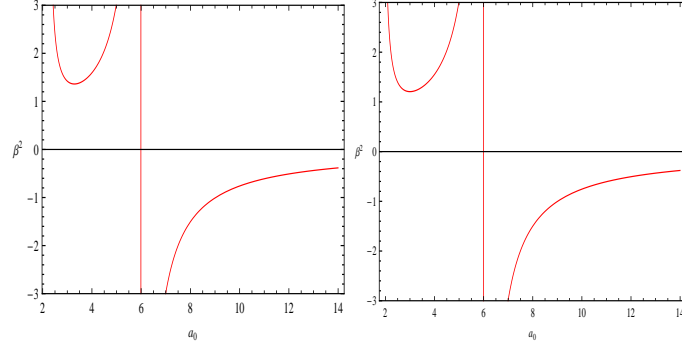


Figure 12: (Color online) Stability regions for thin-shell wormholes corresponding to $\Lambda = -0.5, -0.9$ for fixed values of $Q = 0.1$ and $M = 2$.

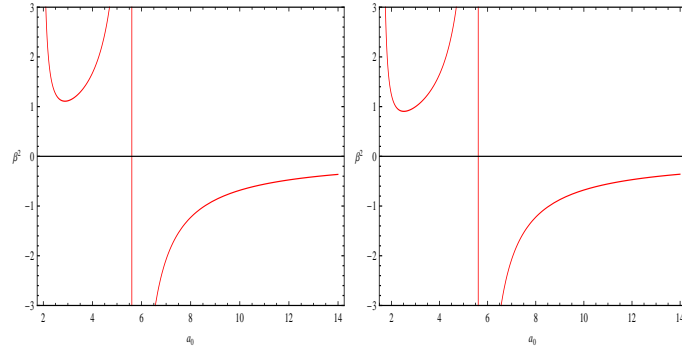


Figure 13: (Color online) Stability regions for thin-shell wormholes corresponding to $\Lambda = -0.5, -0.9$ for fixed values of $Q = 0.7$ and $M = 2$.

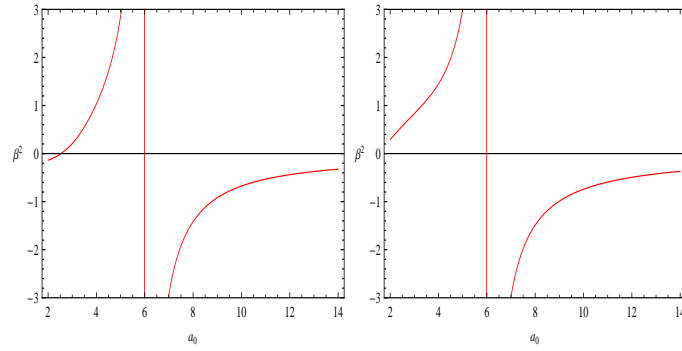


Figure 14: (Color online) Stability regions for thin-shell wormholes correspond to $\Lambda = 0.1, 0.9$ for fixed values of $Q = 0.1$ and $M = 2$.

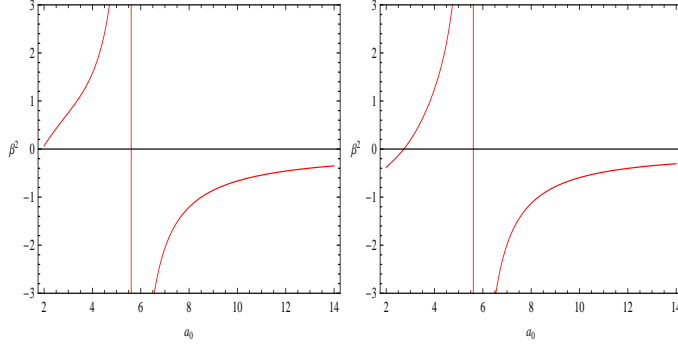


Figure 15: (Color online) Stability regions for thin-shell wormholes correspond to $\Lambda = 0.1, 0.9$ for fixed values of $Q = 0.7$ and $M = 2$

We see that the stability regions can be extended by reducing the value of cosmological constant. Further, we obtain the stability regions by increasing the value of charge and keeping the same value of mass and cosmological constant, i.e., $M = 2$, $Q = 0.7$, $\Lambda = -0.5$ and $M = 2$, $Q = 0.7$, $\Lambda = -0.9$. It is observed that the stability regions increase with the increase of charge which extends to the region $0 < \beta^2 \leq 1$, as shown in Fig. **13**.

On the other hand, we plot stability regions for positive cosmological constant for fixed value of mass and charge. Figure **14** shows the stability regions for $M = 2$, $Q = 0.1$, $\Lambda = 0.1$ and $M = 2$, $Q = 0.1$, $\Lambda = 0.9$. We see from Fig. **15** that the stability regions for $M = 2$, $Q = 0.7$, $\Lambda = 0.1$ and $M = 2$, $Q = 0.7$, $\Lambda = 0.9$ are not of typical form like in the case of negative cosmological constant.

7 Summary

We have studied various aspects of thin-shell wormholes constructed from regular charged black hole with and without cosmological constant in a non-linear electrodynamics field. We have plotted σ and p for different values of parameters M , Q and $a = a_0$ to show the presence of exotic matter confined within the shell of the wormhole. It is observed that the matter distribution is of the phantom energy type in both cases with and without Λ . The nature of the wormhole (attractive and repulsive) has been investigated for fixed values of parameters M and Q . The amount of exotic matter required to support the wormhole is always a crucial issue. We have shown the variation

of exotic matter graphically with respect to charge and mass. It is found that the total amount of exotic matter can be reduced by either decreasing the value of charge or increasing the value of mass.

We have also addressed the issue of stability of thin-shell wormholes subject to linearized radial perturbation around a static solution. For this purpose, the stability regions have been plotted in the form of parameter β . Figures **12-15** show the stability regions to the left and right of the vertical asymptotes for fixed values of M , Q , and Λ . Eiroa⁵⁶⁾ has found that the dilaton thin-shell wormholes have stable configurations in small range as compared to Reissner-Nordström wormholes for the same value of charge. But in both cases, the stable configurations do not lie in the realistic range i.e., $0 < \beta^2 \leq 1$. However, Rahaman et al.¹⁶⁾ and Usmani et al.¹⁷⁾ found the stable configurations in this range. In our case, we have found that the stability regions belong to this range for the case of negative cosmological constant by varying its range for fixed values of charge and mass. This shows the physical relevance of negative cosmological constant on wormhole stability. In other cases, these stable configurations exist similar to Ref.⁵⁶⁾ but do not correspond to the range $0 < \beta^2 \leq 1$ for different values of the parameters.

Acknowledgments

We would like to thank the Higher Education Commission, Islamabad, Pakistan, for its financial support through the *Indigenous Ph.D. 5000 Fellowship Program Batch-VII*. One of us (MA) would like to thank University of Education, Lahore for the study leave.

- 1) N. S. Kardashev: Int. J. Mod. Phys. D **16** (2007) 909.
- 2) E. A. Larranaga: arXiv:gr-qc/0505054v6.
- 3) M. Safonova and D. F. Torres: Mod. Phys. Lett. A **17** (2002) 1685.
- 4) M. S. Morris and K. S. Thorne: Am. J. Phys. **56** (1988) 395.
- 5) M. Visser, S. Kar and N. Dadhich: Phys. Rev. Lett. **90** (2003) 201102.
- 6) M. Visser: Phys. Rev. D **39** (1989) 3182.
- 7) M. Visser: Nucl. Phys. B **328** (1989) 203.
- 8) E. Poisson and M. Visser: Phys. Rev. D **52** (1995) 7318.
- 9) M. Ishak and K. Lake: Phys. Rev. D **65** (2002) 044011.
- 10) C. Armendariz-Picon: Phys. Rev. D **65** (2002) 104010.
- 11) H. Shinkai and S. A. Hayward: Phys. Rev. D **66** (2002) 044005.
- 12) E. F. Eiroa and G. E. Romero: Gen. Relativ. Gravit. **36** (2004) 651.

- 13) F. S. N. Lobo and P. Crawford: *Class. Quantum Grav.* **21** (2004) 391.
- 14) M. Thibeault, C. Simeone and E. F. Eiroa: *Gen. Relativ. Gravit.* **38** (2006) 1593.
- 15) E. F. Eiroa: *Phys. Rev. D* **80** (2009) 044033.
- 16) F. Rahaman, Sk. A. Rahman, A. Rakib and Peter K. F. Kuhfitting: *Int. J. Theor. Phys.* **49** (2010) 2364.
- 17) A. A. Usmani, Z. Hasan, F. Rahaman, Sk. A. Rakib, R. Saibal and Peter K. F. Kuhfitting: *Gen. Relativ. Gravit.* **42** (2010) 2901.
- 18) M. Sharif and M. Azam: *JCAP* **02** (2012) 043; *Gen. Relativ. Gravit.* **44** (2012) 1181; *Eur. Phys. J. C* **73** (2013) 2407.
- 19) M. Visser and D. Hochberg: arXiv gr-qc/9710001.
- 20) S. A. Hayward: arXiv gr-qc/0203051.
- 21) A. Chodos and S. Detweiler: *Gen. Relativ. Gravit.* **14** (1982) 879.
- 22) G. Clement: *Gen. Relativ. Gravit.* **16** (1984) 131.
- 23) K. K. Nandi, B. Bhattacharjee, S. M. K. Alam and J. Evans: *Phys. Rev. D* **57** (1998) 823.
- 24) Y. G. Shen, H. Y. Guo, Z. Q. Tan and H. G. Ding: *Phys. Rev. D* **44** (1991) 1330.
- 25) S. Kar: *Phys. Rev. D* **53** (1996) 722.
- 26) L. A. Anchordoqui and S. E. Perez Bergliaffa: *Phys. Rev. D* **62** (2000) 067502.
- 27) M. Born: *On the Quantum Theory of the Electromagnetic Field*, *Proc. Roy. Soc. Lond. A* **143** (1934) 410; M. Born and L. Infeld, *Foundations of the New Field Theory*, *Proc. Roy. Soc. A* **144** (1934) 425.
- 28) J. F. Plebanski: *Lectures on Non-linear Electrodynamics*, monograph of the Niels Bohr Institute Nordita, Copenhagen (1968).
- 29) E. A. Beato and A. Garcia: *Phys. Rev. Lett.* **80** (1998) 5056.
- 30) E. A. Beato and A. Garcia: *Phys. Lett. B* **464** (1999) 25; *Gen. Relativ. Gravit.* **31** (1999) 629.
- 31) N. Seiberg and E. Witten: *JHEP* **09** (1999) 032.
- 32) M. Novello, S. E. P. Bergliaffa and J. Salim: *Phys. Rev. D* **69** (2004) 127301.
- 33) P. V. Moniz: *Phys. Rev. D* **66** (2002) 103501.
- 34) R. Garcia-Salcedo and N. Breton: *Class. Quantum Grav.* **20** (2003) 5425.
- 35) D. N. Vollick: *Gen. Relativ. Gravit.* **35** (2003) 1151.
- 36) K. A. Bronnikov: *Phys. Rev. D* **63** (2001) 044005.
- 37) I. Dymnikova: *Class. Quantum Grav.* **21** (2004) 4417.
- 38) N. Breton: *Phys. Rev. D* **72** (2005) 044015.

- 39) F. Baldovin, M. Novello, S. E. Perez Bergliaffa and J. M. Salim: *Class. Quant. Grav.* **17** (2000) 3265.
- 40) A. Borde: *Phys. Rev. D* **50** (1994) 3392.
- 41) C. Barrabes and V. P. Frolov: *Phys. Rev. D* **53** (1996) 3215.
- 42) M. Mars, M. M. Martin-Prats and J. M. M. Senovilla: *Class. Quantum Grav.* **13** (1996) L51.
- 43) A. Cabo and E. Ayon-Beato: *Int. J. Mod. Phys. A* **14** (1999) 2013.
- 44) S. W. Hawking and G. F. R. Ellis: *The Large Scale Structure of Space-time*, (Cambridge University Press, 1975).
- 45) W. J. MO, R. G. Cai and R. K. SU: *Commun. Theor. Phys.* **46** (2006) 453.
- 46) H. Salazar, A. Garcia and J. Plebanski: *J. Math. Phys.* **28** (1987) 2171.
- 47) D. Hochberg and M. Visser: *Phys. Rev. D* **56** (1997) 4745.
- 48) G. Darmois: *Memorial des Sciences Mathematiques* (Gauthier-Villars, 1927) Fasc. 25; W. Israel: *Nuovo Cimento B* **44** (1966) 1.
- 49) P. Musgrave and K. Lake: *Class. Quantum Grav.* **13** (1996) 1885.
- 50) M. Visser: *Lorentzian Wormholes* (AIP Press, New York, 1996).
- 51) D. Hochberg and M. Visser: *Phys. Rev. Lett.* **81** (1998) 746; *Phys. Rev. D* **58** (1998) 044021.
- 52) E. F. Eiroa and C. Simeone: *Phys. Rev. D* **71** (2005) 127501.
- 53) T. A. Roman: *Phys. Rev. D* **53** (1993) 5496.
- 54) L. Herrera: *Phys. Lett. A* **165** (1992) 206.
- 55) H. Abreu, H. Hernandez and L. A. Nunez: *Class. Quantum Grav.* **24** (2007) 4631.
- 56) E. F. Eiroa: *Phys. Rev. D* **78** (2008) 024018.